Tribology International xx (xxxx) xxxx–xxxx

Contents lists available at ScienceDirect

Tribology International

journal homepage: www.elsevier.com/locate/triboint

Development of an interactive friction model for the prediction of lubricant breakdown behaviour during sliding wear

Y. Hu, L. Wang*, D.J. Politis, M.A. Masen

Department of Mechanical Engineering, Imperial College London, Exhibition Road, London SW7 2AZ, UK

ARTICLE INFO

Keywords:
Lubricant film breakdown
Pin-on-disc tests
Interactive friction model
Coefficient of friction evolution

ABSTRACT

In this paper, a novel interactive friction-lubricant thickness model was developed to predict the evolution of coefficient of friction and the useful life of lubricant film. The developed model was calibrated by experimental results determined from pin-on-disc tests. For these experiments, a grease lubricant was applied on a Tungsten Carbide ball which slides against a disc made from AA6082 Aluminium alloy. In the pin-on-disc tests, the lubricant film thickness decreased with time during single path sliding leading to a rapid increase in the coefficient of friction. The breakdown of lubricant was divided into three stages, namely, the Stage I low and stable coefficient of friction region, Stage II region in which the coefficient of friction sees a rapid rise, and Stage III in which the coefficient of friction reaches a plateau with a value similar to that of dry sliding. In order to characterise the evolution of coefficient of friction throughout these stages, a novel interactive friction model was developed combining the effects of sliding distance, sliding speed, contact pressure and initial lubricant amount on the evolution of the coefficient of friction. This interactive friction model can be applied to situations involving lubricant breakdown in a dynamic environment such as the metal forming industry, where the use of traditional constant coefficient of friction values present limits in predictive accuracy.

1. Introduction

The study of lubrication breakdown in a lubricated contact has received some attention amongst metal forming researchers due to the growing demand for accurate FE simulation of boundary conditions. In most forming cases, a moderate quantity of lubricant applied between the workpiece and the tool can provide a separation barrier during the metal forming process [1,2]. This amount of lubricant typically involves the assumption of ideal full film lubrication conditions with low coefficient of friction and little wear due to moving objects. However, in many situations, it is not always possible to maintain ideal full film lubrication conditions and there may be considerable levels of non-hydrodynamic lubrication, e.g. boundary lubrication, that result in galling or wear on tooling and the product. This is especially essential for sheet metal forming processes, where the transportation of lubricant is uneven due to the non-uniform distribution of relative sliding distance, strain and contact pressure at the workpiece-tooling interfaces. Moreover, in many cases, lubricant is squeezed out towards regions with lower pressure and side leakage occurs, which will cause further loss of lubricant from the contact and lead to lubricant film breakdown. Therefore, an adequate quantity of lubricant applied prior to the forming operation does not guarantee that lubrication will be effective at all locations or at all stages of a forming operation [2,3].

In recent years, FE simulation has been widely used by metal forming engineers to analyse and optimise forming processes. The coefficient of friction, as one of the key inputs for an FE model, is normally assigned as a constant value [4–7]. However, in practice, lubricant film breakdown might dramatically increase the coefficient of friction, due to the direct contact between the workpiece and dies [8,9]. Classic models that do not take into account changes in the lubrication consistency, may cause inaccuracies in the FE simulation results. Therefore, understanding and modelling the lubricant breakdown behaviour, and the interaction with the evolution of the coefficient of friction and lubricant service life are of great practical importance.

Previously, the phenomenon of lubricant film breakdown has been studied in many fields, including mechanical transmissions [10–12], internal combustion engines [3,13], bearings [14–16] and metal processing [11,17–19]. The influencing factors of lubricant film breakdown have been identified and quantitatively studied. They can be classified into two groups: 1) the operation parameters, including geometry of the contact, sliding speed, load and lubricant amount; and 2) the interface characteristics, including lubricant properties, surface roughness, surface plastic deformation, boundary lubrication and squeezing/side leakage. Bowden and Tabor [3] reviewed the effects of

* Corresponding author.
E-mail address: liliang.wang@imperial.ac.uk (L. Wang).

http://dx.doi.org/10.1016/j.triboint.2016.11.005
Received 26 September 2016; Received in revised form 28 October 2016; Accepted 2 November 2016
Available online xxxx

Please cite this article as: Hu, Y., Tribology International (2016), http://dx.doi.org/10.1016/j.triboint.2016.11.005

speed, lubricant viscosity and temperature on the lubricant breakdown phenomenon in various industrial applications. The sliding speed effects on the mechanism of breakdown were also studied by Begelinger and De Gee [20], in which friction-time diagrams as a function of sliding speed were presented and two important conclusions were drawn: 1) the breakdown time is viscosity dependent and 2) in the low speed region (velocity < 2 m/s), the load-carrying capacity of the lubricant film increases with increasing sliding speed. In Kingsbury's work [14], the effect of increasing lubricant quantity, as extending the running life time before lubricant film breakdown, was observed in ball bearing tests. This effect is also studied by Groche et al. [21,22] and similar conclusions were drawn in metal forming.

As a fundamental study of mechanisms of lubricant film breakdown with the effect from operation parameters, the present paper is concerned with the lubrication of bodies in normal point contact. The aim of this paper is to develop an interactive friction model to characterize the breakdown of the lubricant during sliding point contact and its interaction with the evolution of coefficient of friction. The parameters of lubricant film diminution and breakdown as a function of time and sliding distance due to lubricant transport, sliding speed, load, and the quantity of entrapped lubricant were studied experimentally at room temperature. Based on these results, the interactive relationship between the evolution of the coefficient of friction and the reduction of the lubricant film was modelled, enabling the coefficient of friction and lubricant breakdown to be predicted through a novel friction/film thickness interactive model.

2. Experimental set-up and test programme

Aluminium sheet is studied due to its industrial potential and also lubricated difficulty, which is easy to adhere and be worn [23]. For the production of the disc samples, AA6082 sheet at T6 condition with a thickness of 1 mm was utilised. The mechanical properties of the tested metal are: Young's modulus 72 GPa, Poisson's ratio 0.33, and Vickers hardness 100 HV. The test piece material was cut into squares with dimensions of 50 mm×50 mm. All samples were ground by silicon carbide emery paper to obtain uniform surface roughness. The arithmetic average surface roughness, Ra, was 0.50 (± 0.30) μm, which was measured through a 3D white light interferometry surface profilometer (Veeco Wyko NT9100). The ball material used as the counterpart in the friction tests was Tungsten Carbide WC-6% Co ball (Young's modulus 630 GPa, Poisson's ratio 0.23, Vickers hardness 1780 HV), 6 mm in diameter, due to its good abrasion resistance and low adhesion with aluminium as a potential coating material for aluminium forming [24]. To prevent contamination, both ball and disc were cleaned with acetone and dried in air before the application of lubricant. The lubricant used for the tests was a lubrication grease, OMEGA 35, made from polyethylene glycol, silicon dioxide and graphite. This lubricant features adequate performance in a high temperature environment application (up to 700 °C). The key physical parameters of OMEGA 35 are shown in Table 1.

Two lubricant application methods were used in the friction tests: 1) a precisely controlled quantity of lubricant was applied on the ball to simulate the non-hydrodynamic lubrication (insufficient lubricant) condition and 2) lubricant was evenly applied to the disc to simulate a full film lubrication condition. For condition 1), the lubricant was applied by a dedicated rig designed and manufactured by the authors' group with micro volume lubricant reservoirs of 0.16 μL 0.24 μL, and 0.4 μL, corresponding to an average mass of lubricant applied on the ball of 4 mg, 10 mg and 14 mg, respectively. For the full film lubrication condition, 100 mg of grease was applied on the disc's surface at a thickness of 500 ± 50 μm, which was measured by a plastic wet film comb (Elcometer 3238). The initial lubricated area was assumed to be the projected area of the ball.

Table 1
Lubricant data of OMEGA 35.

Kinematic viscosity (cSt)		Specific gravity (dimensionless)		Dropping point (° C)
40 °C	35	15 °C	1.33	260
100 °C	6			

The frictional behaviour was investigated on an Anton Paar pin-on-disc tribometer under a single direction sliding. The design, measurement and evaluation of tests were partly based on ASTM standards G99. Three sets of tests were designed, aimed at investigating the influence of lubricant transportation and film breakdown phenomenon. The variables are lubricant amount, sliding speed and load. Testing conditions are shown in Table 2 and each condition was repeated three times. The dry sliding test and the full lubricant test (tests no. 1 and 5) were designed for comparing with the steady state coefficients of friction in non-hydrodynamic lubrication. Loads of 0.5, 2 and 5 N were used which corresponded to the mean contact pressure, calculated using Hertz contact theory as, 0.25, 0.4 and 0.55 GPa, respectively. All friction tests were conducted in an ambient environment, at a temperature of 24 °C. The wear track created was analysed by a white light interferometry profilometer (WLI) and an optical microscope to investigate the wear tracks obtained under lubricated and dry conditions to identify the dominant friction mechanism. The coefficient of friction revolution for each test was smoothed. For each condition, different tests were combined and the averages (solid lines) and standard deviations (error bars) are given in Fig. 4.

3. Results and discussion

3.1. Lubrication, friction and wear mechanisms

In the case of insufficient lubrication, the coefficient of friction was low at the initial stage and followed by an abrupt increase of coefficient of friction indicating the breakdown of the lubricant film; finally, the coefficient of friction increases to a stable value similar to the dry contact situation. The results of experiment No. 3 are analysed in Figs. 1–3. The coefficient of friction evolution is shown in Fig. 1 and the wear track is shown in Fig. 2 with the surface topography shown in Fig. 3 after removing the wear debris and the residual lubricant. It is found that the evolution of friction can be divided into 3 stages according to the different coefficient of frictions.

In stage I, the coefficient of friction is low and stable, with an average value of approximately 0.1. No wear scar was observed in this stage (point 1) suggesting that the two surfaces were fully separated by the lubricant film. The friction in stage I may be primarily generated by the internal fluid shear stress of the lubricant at the interface [18]. During sliding, the thickness of the lubricant film gradually decreases due to lubricant transfer from the ball to the aluminium disc and lubrication mode changes from full film lubrication to mixed lubrication regime, which is defined as a transition state between full film lubrication and boundary lubrication and in which two lubrication mechanisms may be functioning [11]. In this mode, the coefficient of friction can be regarded as a constant [3,18].

In stage II, the coefficient of friction starts rising rapidly from about 0.1 and gradually slows down at a value of 0.65. In this regime, the coefficient of friction is highly variable and unstable because the friction stems from fracture phenomena at the surface [3]. At the beginning of stage II, the thickness of lubricant decreases to the height of the peaks on the aluminium surface. In that case, the normal force is supported by both the residual lubricant trapped in the contact and the surface asperities. A wear track develops on the surface, as shown in Fig. 3 point 2 and 3, initially the wear track is almost invisible and becomes wider and deeper with increasing sliding distance. The friction force of this mixed lubrication is supposed to consist of two components: the friction force generated from interacting asperities and the

Table 2
Test matrix.

Effect	Test no.	Temperature	Speed	Load	Mean contact pressure	Lubricant	
						Quantity	Application method
	Unit	°C	mm/s	N	GPa	mg/mm^2	
Lubricant amount	1	24	10	5	0.55	0 (dry)	No lub
	2	24	10	5	0.55	0.2	On the ball
	3	24	10	5	0.55	0.5	On the ball
	4	24	10	5	0.55	0.7	On the ball
	5	24	10	5	0.55	4 (full film)	On the disc
Speed	6	24	30	5	0.55	0.5	On the ball
	7	24	50	5	0.55	0.5	On the ball
Load	8	24	10	0.5	0.25	0.5	On the ball
	9	24	10	2	0.4	0.5	On the ball

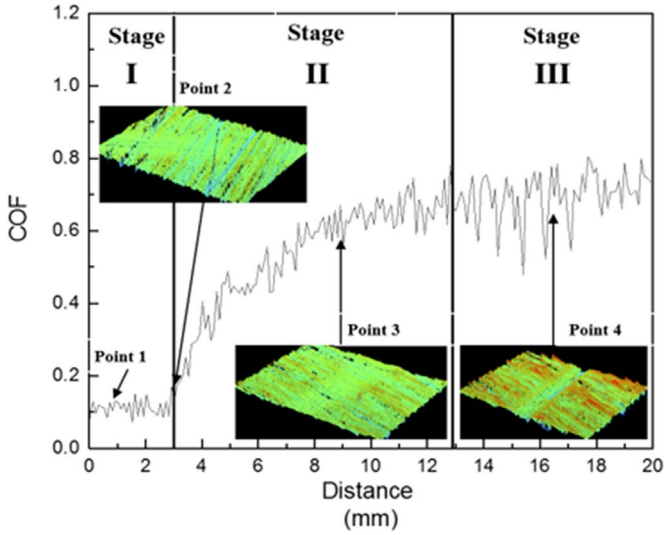

Fig. 1. Evolution of the coefficient of friction (10 mm/s, 5 N/0.55 GPa and 0.2 mg/mm^2) with the local wear track images obtained using WLI at different sliding distances. The image shows 4 points chosen from different stages in the friction curve. The wear track becomes more obvious with increasing sliding distance and COF.

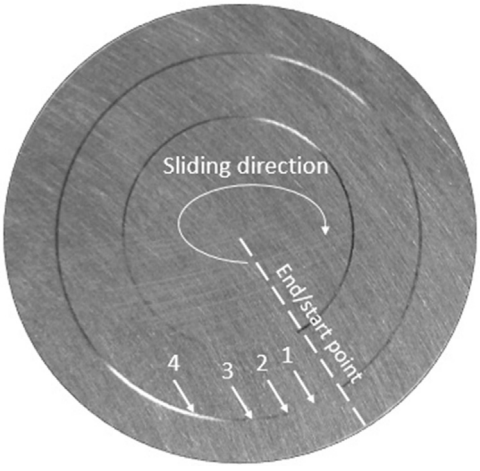

Fig. 2. Wear tracks on the disc within one lap of sliding wear, with the locations of points 1–4 marked on the disc.

shearing of the remaining lubricant [25]. The interacting asperities friction was mainly caused by deformation and explained as the asperities deform and fracture into wear particles, which are entrapped and generate ploughing tracks as the ball penetrated into and moved along the wear track. It was found that the adhesive friction between

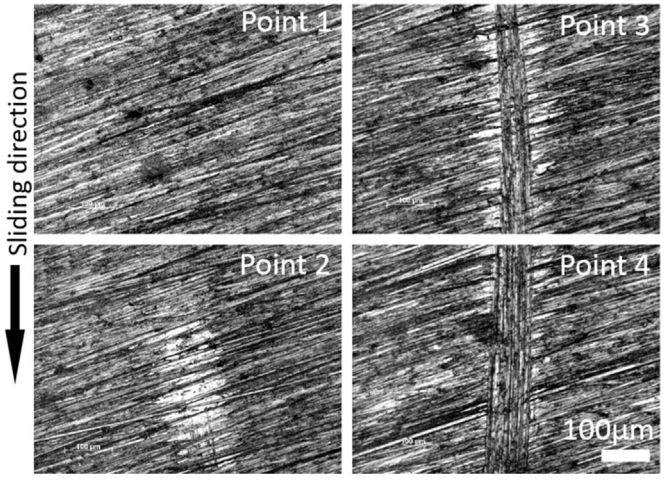

Fig. 3. Wear track topography at different sliding distances.

the WC-Co 6% ball and the aluminium alloy disc did not play an important role in the present research since the material transfer between them was hardly observed by a microscope in the tested sliding distance. Both stage II and III were dominated by ploughing friction due to the large hardness difference between WC and aluminium: the disc surface was ploughed by the hard asperities on the WC ball as well as the wear debris. The width of the wear track on the aluminium surface increases in this stage (Fig. 3 point 2, 3, 4) because the effects of residual lubricant become less significant as the sliding distance increases.

In stage III, the coefficient of friction reaches a plateau with an average value of 0.65, which was close to that obtained under dry sliding. The fluctuation of the coefficient of friction was severe. In this stage, the lubricant is almost completely removed from the contact interface and hence ploughing friction played an important role in the overall friction force. With the severe ploughing damage on the surface (Fig. 3 point 4), many large sized wear particles were generated and entrapped in the wear track during sliding wear. It was expected that the quantity and size of the particles generated on the track reached a dynamic balance, which may indicate that the quantity of entrapped particles was equal to that being ejected from the wear track, leading to a relative stable third body condition and a stable coefficient of friction [4].

3.2. Evolution of coefficient of friction during the sliding wear between lubricated contact pairs

The effects of applied lubricant quantity, load and sliding speed on the lubricant breakdown distance and coefficient of friction were studied experimentally. The experimental data for different quantities

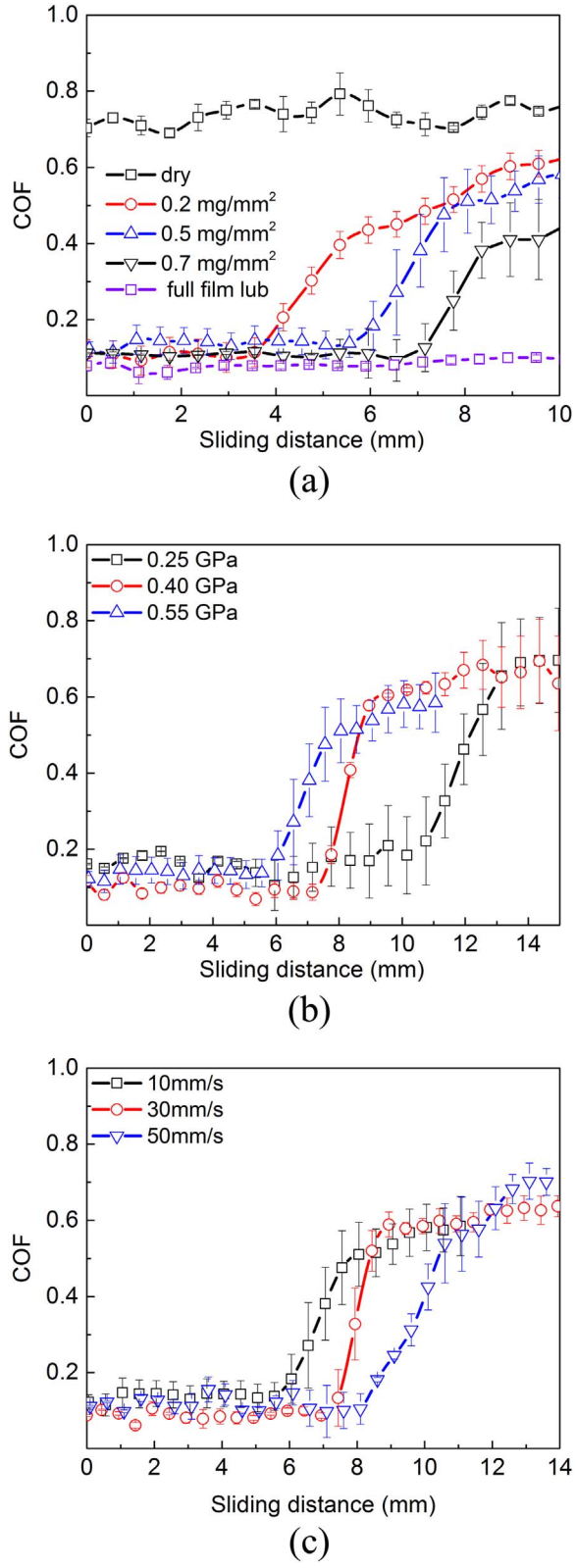

Fig. 4. Coefficient of friction evaluations showing the effects of: (a) quantity of lubricant, (b) contact pressure (c) sliding speed.

of applied lubricant are shown in Fig. 4(a). As can be seen, it was found that the increase in lubricant quantity (from 0.2 mg/mm^2 to 0.7 mg/mm^2) leads to an increased sliding distance at which low friction is experienced. As expected, in the dry sliding and fully lubricated tests, there was no coefficient of friction transition observed. It is therefore indicated that the length of the stage I region was influenced by the initial lubricant quantity that was entrapped at the interface, that is, the reduced lubrication quantity diminished the operating time before lubricant breakdown. This conclusion agrees with previous researchers' work [2,14,19].

An examination of the effect of load, as shown in Fig. 4(b), demonstrates that the distance of lubricated stage I becomes shorter as the pressure increases from 0.25 to 0.55 GPa. This breakdown phenomenon agrees with the trend predicted from the generalised Stribeck curve and the Sommerfeld number, $\frac{\eta v}{P}$ (where η is the viscosity of lubricant, v is the sliding velocity and P is the load) [3,26], that is, the increasing load will result in thinner lubricant film and thus premature breakdown. According to the International Research Group (IRG) transition diagram [20,27,28], a similar conclusion can be drawn: an increase of the load will lead to a decrease of the load-carrying capability of a lubricant and cause earlier onset of the primary transition in film failure.

As shown in Fig. 4(c), the effect of sliding speed (10 mm/s, 30 mm/s and 50 mm/s) on the evolution of coefficient of friction was investigated. An elongation of the breakdown distance with increasing sliding speed was observed in the film breakdown test: the longest low-friction regime is obtained from the test of 50 mm/s. This may be due to the fact that an increased sliding speed will increase the film thickness [17,18,29,30] as the contact fully immersed in lubricant. This analysis of film breakdown mechanism is probably only virtue of the fact that the speed of sliding is lower than a threshold value due to the temperature influence. Begelinger and De Gee [20] found that, at a low speed (v < 2 m/s), the increase of sliding speed will increase the load-carrying capability and thus extend the film breakdown distance; however, a contrast phenomenon, showing a load-carrying capability decrease with higher speed (v > 2 m/s). A similar phenomenon that the increase of sliding speed will decrease wear of the contact was recorded by Bowden and Tabor [3] in a piston/cylinder reciprocation test. It was explained as the amount of hydrodynamic lubrication is greatly increased with increasing speed. The contrast experimental observations may be caused by the temperature increase during high speed sliding and lubricant failure.

4. Interactive friction modelling of lubricant behaviour

Based on Bowden and Tabor [3] and later Azushima's models [31], the overall coefficient of friction, μ, generated between the WC-6% Co ball and the lubricated aluminium disc stems from two mechanisms (Eq. (1)), namely the coefficient of friction at the full film lubrication condition, μ_L, and the dry coefficient of friction, μ_d. In the present work, the contribution of these two components are decided by a lubricated area ratio, β, which various from 0 (the initial full lubricated state) to about 1 (dry sliding state).

$$\mu=(1-\beta)\mu_L+\beta\mu_d \quad (1)$$

As discussed, the contact evolved from the initial full film lubrication to eventual dry sliding during the sliding process. This process could be separated into three components: 1) the initial full lubrication state with a low coefficient of friction, 2) the transition to mixed lubrication condition or eventually boundary lubrication with the increasing of coefficient of friction and 3) the dry sliding condition, in which the coefficient of friction stabilized at a high value. Therefore, it may be reasonable to assume constant values of coefficient of friction, i.e. μ_L=0.13 and μ_d=0.6, for the initial full lubricated and final dry sliding states, whose values can be determined from the friction tests under full film lubrication and dry sliding conditions. It is claimed that the lubrication states, determined by the film thickness, give different coefficients of friction and the decrease of lubricant film thickness gives more chance of solid contact and thus increase the friction [11,18]. This relationship, between the film thickness, $h(t)$ and the lubricated area ratio, β, is modelled by Eq. (2), where $h(t)$ is the instantaneous

film thickness of the lubricant to represent the friction transferring from a steady stage to a breakdown stage, and λ_1 and λ_2 are breakdown distance parameters for the lubricant.

$$\beta=\exp\ [-(\lambda_1 h(t))^{\lambda 2}] \tag{2}$$

In the experiment, the thickness of the lubricant film, $h(t)$, is primarily influenced by the transportation of lubricant during sliding, entrapped lubricant quantity, lubricant squeezed out, sliding speed, lubricant properties and contact geometry. By incorporating the operational parameters, and assuming a constant volume case where the volume of initial entrapped lubricant is equal to the volume smeared on the track, a lubricant film thickness model with variable sliding speed v, Hertz contact radius r, initial film thickness $h(0)$, and instantaneous film thickness $h(t)$ can be developed and is presented in Eq. (3).

$$Ah(0)=Ah(t)+\sqrt{A}\int_0^t f(P,\quad \eta)h(t)v^{\kappa 1}dt \tag{3}$$

where $A$is the area of the Hertzian circle and the boundary condition is found when t=0, $h(t)=h(0)$. As the amount of entrapped lubricant is determined by the thickness and the lubricant properties, and is nearly independent of the size of the deformed region [32], a constant Hertzian contact area is assumed. $Ah(0)$ is the initial volume of the entrapped lubricant, $Ah(t)$ is the entrapped volume at time t and $\sqrt{A}\int_0^t h(t)v^{\kappa 1}dt$ is the volume of lubricant transported onto the wear track during sliding (Fig. 5).

The volume of lubricant smeared on the track during sliding is calibrated by the function, $f(P, \eta)$, where P is the mean contact pressure calculated by the Hertz contact equations [33]; and η is the viscosity of the lubricant, which is assumed as a constant at room temperature. Thus $f(P, \eta)$ can be written as $f(P, \eta)=b \times P^{\kappa 2}$, where b is a constant. Therefore, Eq. (3) incorporates additional operating parameters compared to equations used in previous studies [30,34], who's efforts focused on the effect of lubricant squeezed out of the contact surface only as a function of pressure and load for a given lubricant. This equation can be transferred into a first order linear differential equation (Eq. (4)) (the area A is integrated into constant c).

$$\dot{h}(t)=\frac{dh}{dt}=-h(cP^{\kappa 1}v^{\kappa 2}t) \tag{4}$$

In Eq. (4), c, κ_1 and κ_2 are breakdown time parameters that can be determined from the friction evolution curve; c is a friction constant; P is the contact pressure and u is the sliding speed. This instantaneous film thickness equation can be integrated into the form of Eq. (5) by solving the boundary conditions: $h(t)=h(0)$ at time t=0.

$$h(t)=h(0)\exp[-cP^{\kappa 1}v^{\kappa 2}t] \tag{5}$$

The right side of Eq. (5) may be divided into two components: $h(0)$ and exp $[-cP^{\kappa 1}v^{\kappa 2}t]$, which indicate the initial film thickness and the film diminution rate respectively. The variables of diminution rate (P and v) are represented by Power Law, with similar form of Dowson's equations [35–37]. The breakdown time was calculated using Eq. (4). The highest asperity peak was approximately 1 μm. Thus, when the lubricant thickness, $h(t)$, is smaller than the asperity's height, breakdown would occur [11,38] and the parameters, c, κ_1 and κ_2, can be determined. It has to mention that this assumption is simple and relatively accurate. Some advanced studies show complex effects of surface roughness on lubricant breakdown [39,40], which are not intended to cover in this study. $h(0)$ is assumed to be determined only by the quantity of applied lubricant. The initial lubricant film thickness, $h(0)$ = 12 μm, is set based on the condition of 0.5 mg/mm^2 lubricant applied. The $h(0)$ values for application volumes of 0.3 mg/mm^2 and

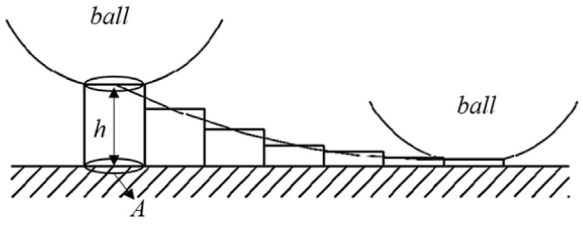

Fig. 5. Schematic model of lubricant transportation with an initial thickness of h and area of A.

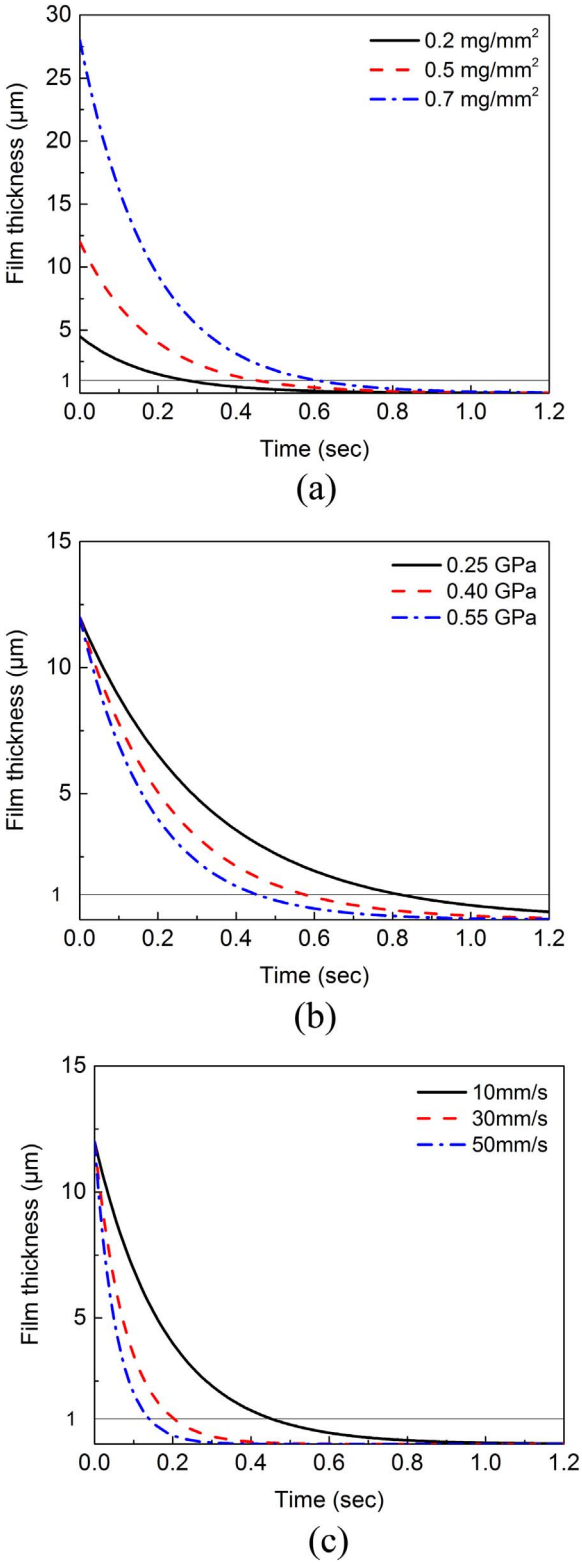

Fig. 6. Simulation results of lubricant film thickness diminution under various (a) lubricant quantity, (b) load and (c) sliding speed.

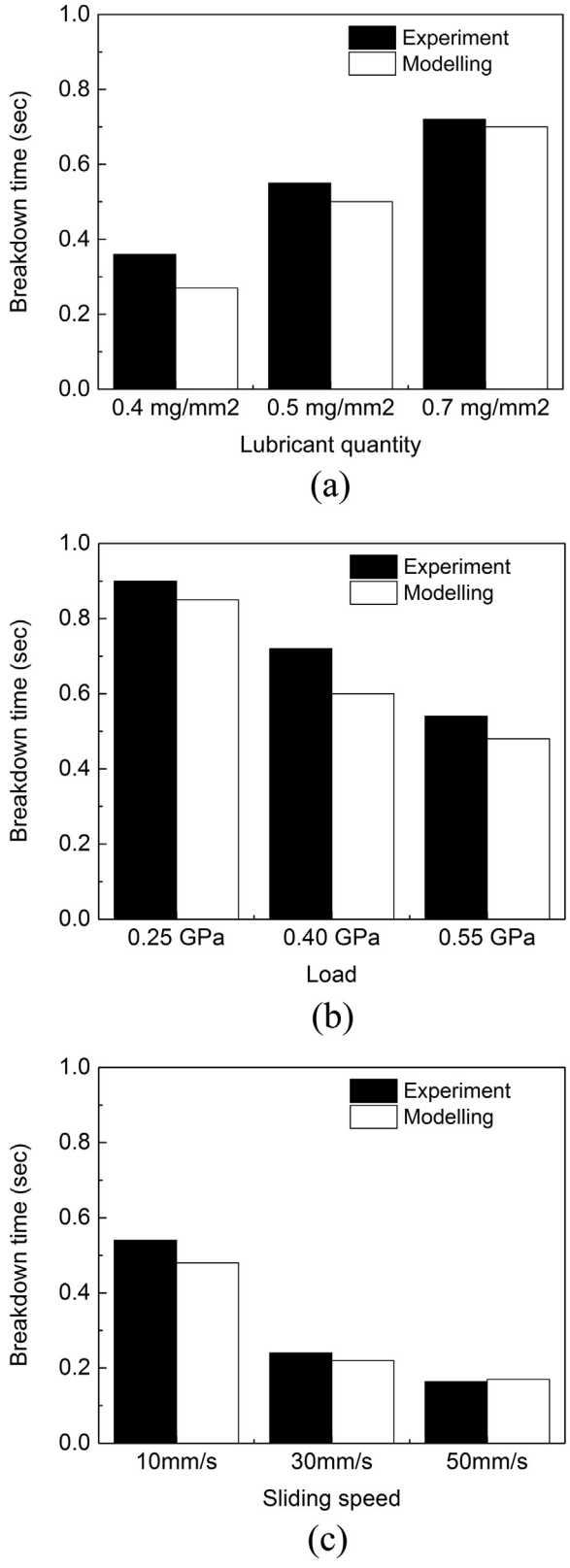

Fig. 7. Comparison of simulation and experiment result of breakdown time under various (a) lubricant quantity, (b) load and (c) sliding speed.

0.7 mg/mm^2 are calculated from this pre-setting value, which are 4.5 and 28 μm. The friction model was calibrated using the obtained experimental data. The calibration consists of two steps:

1) The breakdown time was calibrated using Eq. (4). The parameters, c, κ_1 and κ_2 , can be determined from the experimentally observed breakdown time.
2) With the film thickness obtained from step 1, the coefficient of friction evolution is fitted by Eqs. (1 and 2) with the parameters λ_1 and λ_2 determined from the breakdown distance.

Table 3
Model constants and model parameters of the interactive friction model.

Unit	λ_1	λ_2	κ_1	κ_2	C
	μm^{-1}	–	–	–	s_2^{k-1} $GPa^{-k}{}_1$ $mm^{-k}{}_2$
	3	2.3	0.75	0.73	1.6

The processes of determining these parameters and the modelling results of lubricant film thickness with respect to time are shown in Fig. 6. Comparisons between modelling and experimental results are shown in Fig. 7, indicating that the interactive friction model enables the prediction of breakdown time of lubricant film. The model parameters and constants are listed in Table 3, which were determined by using a dedicated algorithm developed in the authors' group. After the constants have been determined, the model can be used to predict the evolution of coefficient of friction under a range of conditions. The interactive friction model developed in the present paper is valid for the prediction of the coefficient of friction evolutions for loads between 0.5 and 5 N and sliding speed between 10 mm/s and 50 mm/s.

Comparison with other lubricant film thickness results are discussed in this section. The Eq. (4) is similar to the Wilson's lubricant film thickness model [6,38,41,42] in the form of ODEs. Wilson's model was developed on Reynolds equation in sheet metal forming simulation. The film thicknesses calculated from Eq. (4) have been compared with experimental measurement (in dome test) and various theoretical predictions shown in Fig. 8. The model developed in this paper enables the description of typical evolution curves observed in previous research, i.e. an initial rapid decrease in film thickness followed by a gradual reduction in thickness. The present film thickness model shows its flexibility for modelling lubricant transportation and squeezing out phenomena. Also, this model shows the ability that the lubricant film can diminish to the height of asperity as a result of non-hydrodynamic lubrication, comparing to other results and models under the full film lubrication condition and assumption that the lubricant film thicknesses finally reduce to constant values as full film lubrications are obtained.

The fitting results between predicted and experimentally obtained coefficient of friction evolutions are shown in Fig. 9. Good agreements

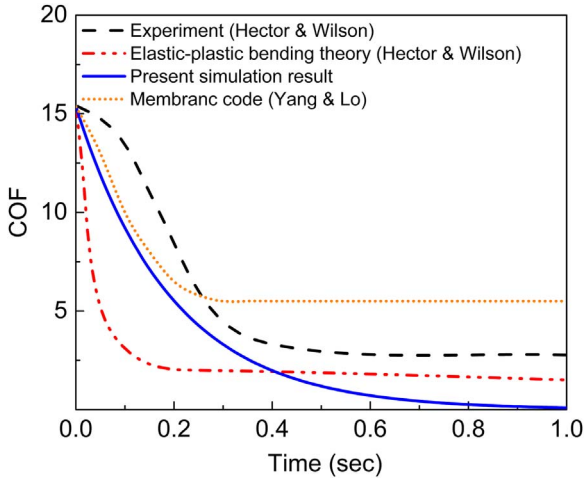

Fig. 8. Comparison of various theoretical predictions (elastic-plastic bending theory [6]; Membrane code [5]) with Hector and Wilson's measurements [42] of film thickness.

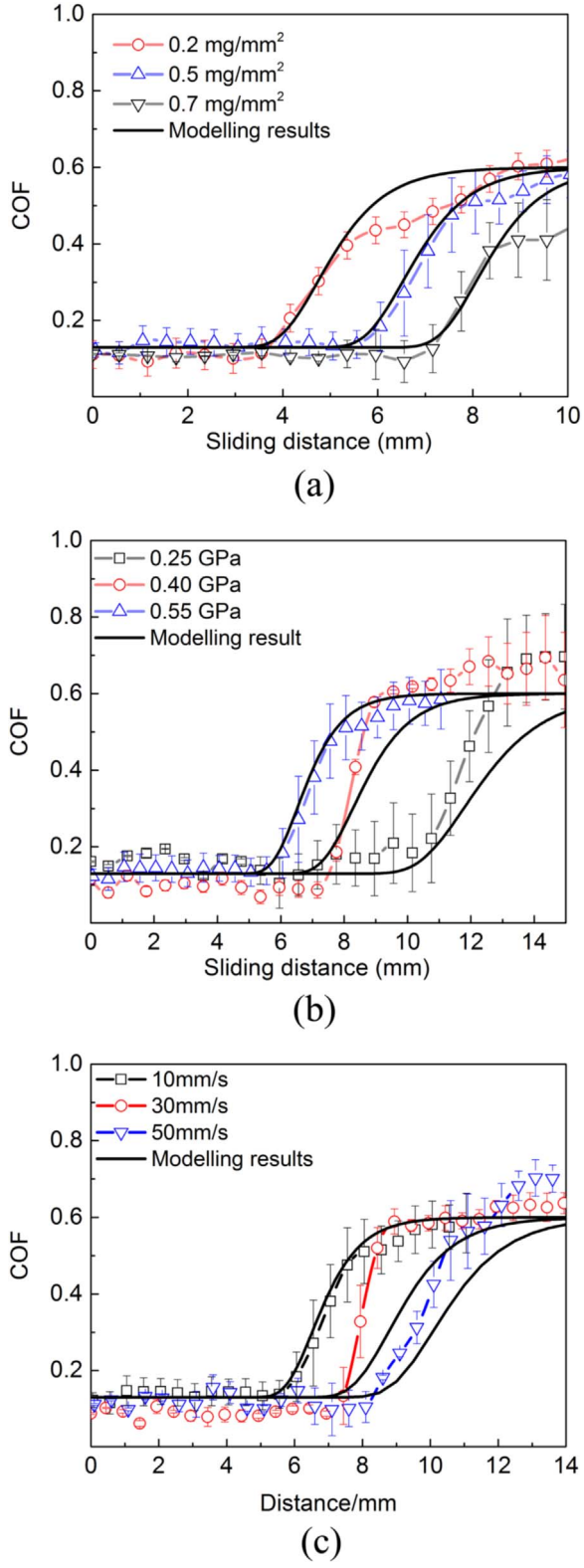

Fig. 9. Comparison of modelling and experiment result of coefficient of friction evolution under various (a) lubricant quantity, (b) load and (c) sliding speed.

have been achieved. In addition, a three dimensional friction/lubricant regime transfer diagram has been generated, as shown in Fig. 10. The stage transfer and relative coefficient of friction can be predicted with certain operation parameters (lubricant amount, sliding speed and load). The breakdown distance is also determined as a function of sliding speed and load. With the increase of sliding distance (z-axis),

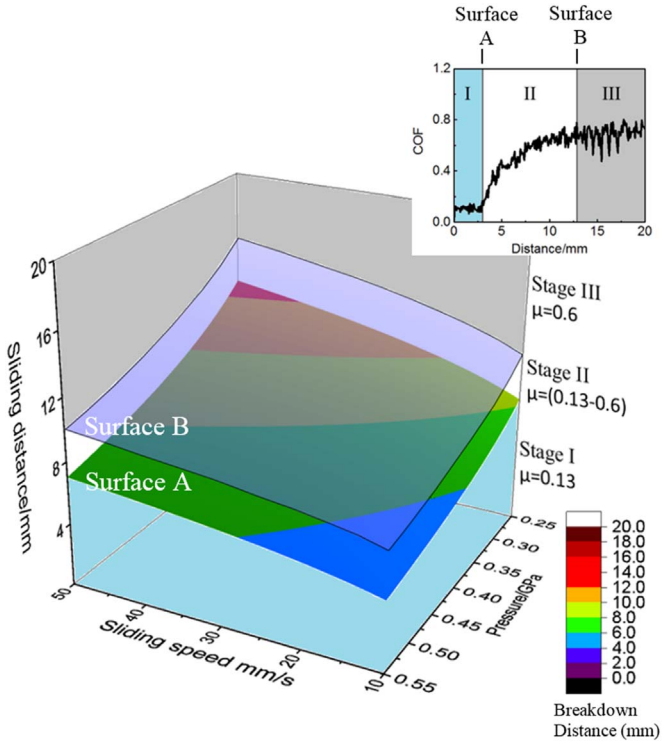

Fig. 10. Three dimensional representation of the modelling result: lubricant behaviour window at 0.5 mg/mm^2 condition.

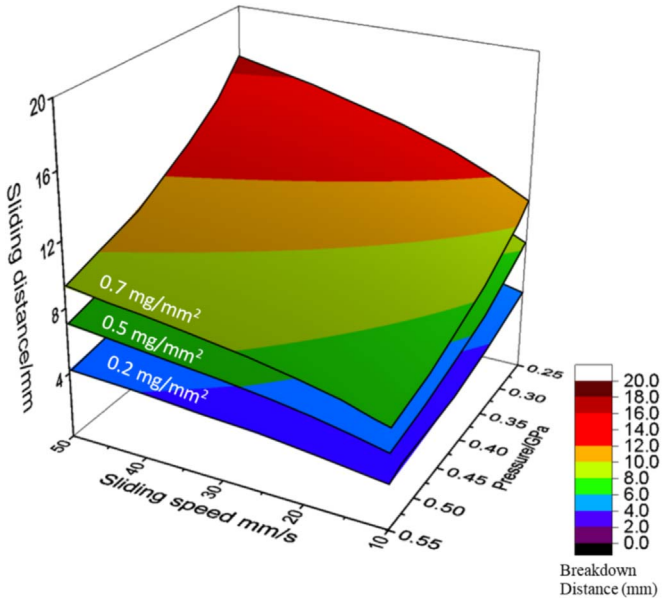

Fig. 11. Lubricant behaviour window: breakdown distance surfaces of different initial lubricant quantity applied.

the coefficient of friction increases from 0.13 to 0.6, corresponding to the transition from stage I to stage III. The surfaces, A and B, indicate the boundary of different stages. Furthermore, a lubrication behaviour window of the lubricant can be obtained to predict the full film lubrication region in case of lubricated wear (Fig. 11). The setting of operation parameters under the breakdown distance surfaces are desired full film lubrication and low coefficient of friction are obtained in this region. In this figure, the condition of high speed (50 mm/s), low pressure (0.25 GPa) and large lubricant amount (0.7 mg/mm^2) gives the longest breakdown distance (18 mm).

5. Conclusions

In the present research, an interactive friction model has been developed to characterize the lubricant film breakdown phenomena. The effects of lubricant thickness, sliding speed and contact pressure on the evolution of friction coefficient have been studied and the novel interactive friction model has enabled the prediction of friction coefficient evolution as a function of sliding distance. From the work performed in the paper, the following conclusions can be drawn:

1) The pin-on-disc test results illustrate that the friction evolution process of a grease lubricated sliding contact comprises of three stages corresponding to different friction mechanisms, namely a stage I with full film lubrication and low coefficient of friction, stage II with sharp increasing coefficient of friction, and stage III, a steady stage with a high coefficient of friction.
2) Lubricant regime transformation plays an important role in the sliding friction process. The gradual decrease of lubricant film thickness causes a transformation from full film lubrication to boundary lubrication and the development of surface damage which marks the beginning of stage II.
3) The interactive friction/film thickness model developed in the present research provides an effective method to predict the film breakdown time and distance at different lubricant amount, load, and sliding speed, and thus allows for modelling of the lubricant film breakdown phenomenon that occurs in the sliding process.

Acknowledgements

The research in this paper was supported by the European Commission 7th Framework Programme (Grant agreement no: 604240) as part of the project 'LoCoLite: An industry system enabling the use of a patented materials processing technology for Low Cost forming of Lightweight structures for transportation industries' and the Horizon 2020 Research and Innovation Programme (Grant agreement no. 723517) as part of the project 'LoCoMaTech: Low Cost Materials Processing Technologies for Mass Production of Lightweight Vehicles'. This research was also supported by the China Scholarship Council (Grant CSC no. 201406120074): A non-profit institution enabling talented Chinese students to undertake a PhD programme overseas.

References

[1] A.D. Foster, et al., An investigation of lubrication and heat transfer for a sheet aluminium heat, form-quench (HFQ) process, Steel Res Int 79 (2008) 133–140.
[2] W. Wilson, Friction and lubrication in bulk metal-forming processes, J Appl Metalwork 1 (1) (1978) 7–19.
[3] F.P. Bowden, D. Tabor, The friction and lubrication of solids 1, Oxford university press, Oxford, 2001.
[4] G. Ma, et al., The friction coefficient evolution of a TiN coated contact during sliding wear, Appl Surf Sci 345 (2015) 109–115.
[5] T.-S. Yang, S.-W. Lo, A finite element analysis of full film lubricated metal forming process, Tribol Int 37 (8) (2004) 591–598.
[6] T.-C. Hsu, W.R. Wilson, Refined models for hydrodynamic lubrication in axisymmetric stretch forming, J Tribol 116 (1) (1994) 101–109.
[7] W. Wang, et al., A study on variable friction model in sheet metal forming with advanced high strength steels, Tribol Int 93 (2016) 17–28.
[8] D.-W. Zhang, H. Ou, Relationship between friction parameters in a coulomb – tresca friction model for bulk metal forming, Tribol Int 95 (2016) 13–18.
[9] A. Clarke, et al., Running-in and micropitting behaviour of steel surfaces under mixed lubrication conditions, Tribol Int 101 (2016) 59–68.
[10] J. Castro, J. Seabra, Scuffing and lubricant film breakdown in FZG gears part I, analytical and experimental approach, Wear 215 (1) (1998) 104–113.
[11] B. Bhushan, Introduction to tribology, John Wiley & Sons, Chichester, 2013.
[12] X. Fang, et al., Industrial gear oil – a study of the interaction of antiwear and extreme-pressure additives, Tribol Int 26 (6) (1993) 395–398.
[13] E. Tomanik, Friction and wear bench tests of different engine liner surface finishes, Tribol Int 41 (11) (2008) 1032–1038.
[14] E. Kingsbury, Lubricant-breakdown in instrument ball bearings, J Lubr Technol 100 (3) (1978) 386–393.
[15] D. Sander, et al., Simulation of journal bearing friction in severe mixed lubrication – validation and effect of surface smoothing due to running-in, Tribol Int 96 (2016) 173–183.
[16] X. Shi, L. Wang, F. Qin, Relative fatigue life prediction of high-speed and heavy-load ball bearing based on surface texture, Tribol Int 101 (2016) 364–374.
[17] K. Holmberg, A. Matthews, Coatings tribology: properties, mechanisms, techniques and applications in surface engineering tribology series 56, Elsevier Science and Technology Books, Oxford, UK, 1994.
[18] S. Wen, P. Huang, Principles of tribology, John Wiley & Sons, Singapore, 2012.
[19] W. Wilson, W. Carpenter, A thermal hydrodynamic model for the lubrication breakdown in upsetting between overhanging dies, Wear 24 (3) (1973) 351–360.
[20] A. Begelinger, A. De Gee, Failure of thin film lubrication – a detailed study of the lubricant film breakdown mechanism, Wear 77 (1) (1982) 57–63.
[21] P. Groche, J. Stahlmann, C. Müller, Mechanical conditions in bulk metal forming tribometers – part two, Tribol Int 66 (2013) 345–351.
[22] P. Groche, et al., Mechanical conditions in bulk metal forming tribometers – part one, Tribol Int 62 (2013) 223–231.
[23] X. Fan, L. Wang, Ionic liquids gels with in situ modified multiwall carbon nanotubes towards high-performance lubricants, Tribol Int 88 (2015) 179–188.
[24] Dong Y, Li X, Dong H. Techniques for design and manufacture of surface engineered tools for HFQ aluminium. LoCoLite Project Report; 2015.
[25] E. Gelinck, D. Schipper, Calculation of stribeck curves for line contacts, Tribol Int 33 (3) (2000) 175–181.
[26] D.J. Schipper, Transitions in the lubrication of concentrated contacts, University of Twente, Enschede, The Netherlands, 1988 [Ph.D thesis].
[27] G. Salomon, Failure criteria in thin film lubrication – the IRG program, Wear 36 (1) (1976) 1–6.
[28] D. Schipper, A. De Gee, Lubrication modes and the IRG transition diagram, Lubr Sci 8 (1) (1995) 27–35.
[29] Y. Chiu, An analysis and prediction of lubricant film starvation in rolling contact systems, ASLE Trans 17 (1) (1974) 22–35.
[30] L.D. Wedeven, D. Evans, A. Cameron, Optical analysis of ball bearing starvation, J Tribol 93 (3) (1971) 349–361.
[31] A. Azushima, Recent development and theory of lubrication in cold sheet rolling, Tetsu-to-Hagane 64 (1978) 317–330.
[32] Archard J, Kirk M. Lubrication at point contacts. In: Proceedings of the royal society of London A: mathematical, physical and engineering sciences. The Royal Society; 1961.
[33] K.L. Johnson, K.L. Johnson, Contact mechanics, Cambridge university press, Cambridge, 1987.
[34] Dowson D, Whomes T. Paper 8: side-leakage factors for a rigid cylinder lubricated by an isoviscous fluid. In: Proceedings of the institution of mechanical engineers, conference proceedings. SAGE Publications; 1966.
[35] B.J. Hamrock, D. Dowson, Isothermal elastohydrodynamic lubrication of point contacts: part II – ellipticity parameter results, J Lubr Technol 98 (3) (1976) 375–381.
[36] B.J. Hamrock, D. Dowson, Isothermal elastohydrodynamic lubrication of point contacts: part III – fully flooded results, J Lubr Technol 99 (2) (1977) 264–275.
[37] B.J. Hamrock, D. Dowson, Isothermal elastohydrodynamic lubrication of point contacts: part IV – starvation results, J Lubr Technol 99 (1) (1977) 15–23.
[38] W. Wilson, T. Hsu, X. Huang, A realistic friction model for computer simulation of sheet metal forming processes, J Eng Ind 117 (2) (1995) 202–209.
[39] I. Krupka, P. Sperka, M. Hartl, Effect of surface roughness on lubricant film breakdown and transition from EHL to mixed lubrication, Tribol Int 100 (2015) 116–125.
[40] J. Lundberg, Influence of surface roughness on normal-sliding lubrication, Tribol Int 28 (5) (1995) 317–322.
[41] W. Wilson, J. Wang, Hydrodynamic lubrication in simple stretch forming processes, J Tribol 106 (1) (1984) 70–77.
[42] L. Hector, W. Wilson, Hydrodynamic lubrication in axisymmetric stretch forming – part 2: experimental investigation, J Tribol 113 (4) (1991) 667–674.